

4

Theoretical and Experimental Research: Diagnostic Analysis of the Feed Kinematic Chain Mechanical System

4.1 INTRODUCTION TO MECHANICAL SYSTEMS ANALYSIS

The dynamic study of a mechanical system has as its goal the knowledge and, sometimes, the prediction of the dynamic behavior, in order to understand which way the modifications made to a system or to the disturbing sources affect the dynamic behavior of this system. Physical or mathematical models must be created in this respect, models that can approximate as well as possible the behavior of the real system.

The creation of a system model usually supposes the use of an adequate combination of theoretical and experimental methods whose succession is determined by the goals of the research and the characteristics of the system. Theoretical analysis of the system is carried out to determine the dynamic properties of the system and is based on equations that characterize the system, also known as “model construction equations.” The theoretical analysis implies certain steps that must be followed:

1. Establishing some simplifying hypothesis for the system in order to reduce the analysis effort

2. Establishing the sum equations for the masses, the energies, and/or the impulses that occur in the system
3. Establishing the phenomenological equations in the case of irreversible processes (i.e., heat propagation)

Generally, a system of ordinary differential and/or partial derivative equations is obtained, and these equations represent the theoretical model of the system of given structure and parameters. This model is frequently very complex and can not be used as it is. Model simplification is necessary and can be accomplished by

Linearization of partial derivative equations

Approximation by ordinary differential equations of the partial derivative equations

Reduction of the order of ordinary differential equations

The resulting theoretical model contains the functional link between the physical data of the system and its parameters. The theoretical model is recommended only if sufficient elements are known (elements that are connected to the laws that characterize the system's dynamic behavior), or if the theoretical model's behavior must be simulated. It must be stressed that theoretical analysis enables the researcher to establish equations that describe the dynamics of the modeled system even when the system is in the state of design, not available for experiments.

Experimental analysis of a system, a method also known as "identification of the system," proposes to determine the mathematical model on the basis of measurements of variables that characterize its evolution in a certain regime. In this situation, we always start from knowledge about the system gathered through previous theoretical or other analysis. Then, the input and output of the system are measured and evaluated using an adequate method for identification, which is the link between the measured variables. It should be noted that the input magnitudes can be signaled by the normal function of the system or can be artificially introduced signals. The experimental model contains numerical values as parameters whose functional connection with the physical data remains unknown. This model, which generally describes the momentary dynamic behavior of the system, is obtained with minimal effort, and can be used to lead or predict certain variables.

Theoretical analysis can use the results of the experimental analysis to verify the precision of the theoretical model or to determine the parameters of the model that cannot be determined otherwise. The

experimental analysis can use the results of the theoretical analysis especially for the model structure.

The models that result from the two types of analysis can be compared. Reexecuting certain steps of the analysis can eliminate the eventual nonconcordances.

In conclusion, it is evident that the correct model of a system is necessary to perform an adequate combination of theoretical and experimental methods. One of the possible combinations of the two types of analysis is presented in [Figure 4.1](#). The analysis steps and their succession are influenced during the procedure.

4.2 THE EXPERIMENTAL STAND

The kinematic feed chain ensures the cyclical positioning on one of the generating trajectories (G, D) of the generator element (D_E or G_E). The classical structure of the kinematic feed chains is presented in [Figure 4.2](#), where the notations represent the following.

OP represents the start/stop of machine movement.

I is the reverse for the feed movement direction.

Ks is the mechanism of periodic transmission of the movement (if the advance is intermittent).

M_R is the mechanism of feed magnitude adjustment.

S is the safety mechanism (protection to overloads).

M_T is the mechanism that transforms the rotation movement into translation movement.

In the most recently proposed structures of the feed kinematic chains some of the above-presented mechanisms have disappeared, their roles being taken by the driving element which is usually a continuous current motor with a large domain for rpm adjustment.

The problem of establishing the technical diagnostic in the kinematic feed chains of modern machine tools necessitated building an adequate testing stand, one that contained all the necessary elements. [Figure 4.3](#) presents the structural kinematic schema of the studied kinematic feed chain.

The driving element is a direct current motor, type SMUC-35, having the characteristics:

The actual moment, $M_n = 35 \text{ Nm}$

The nominal intensity of current, $I_n = 28 \text{ A}$

The couple with the ampere coefficient, $K_T = 13 \text{ Nm/A}$

The inertial moment, $j = 0.065 \text{ kgm}^2$

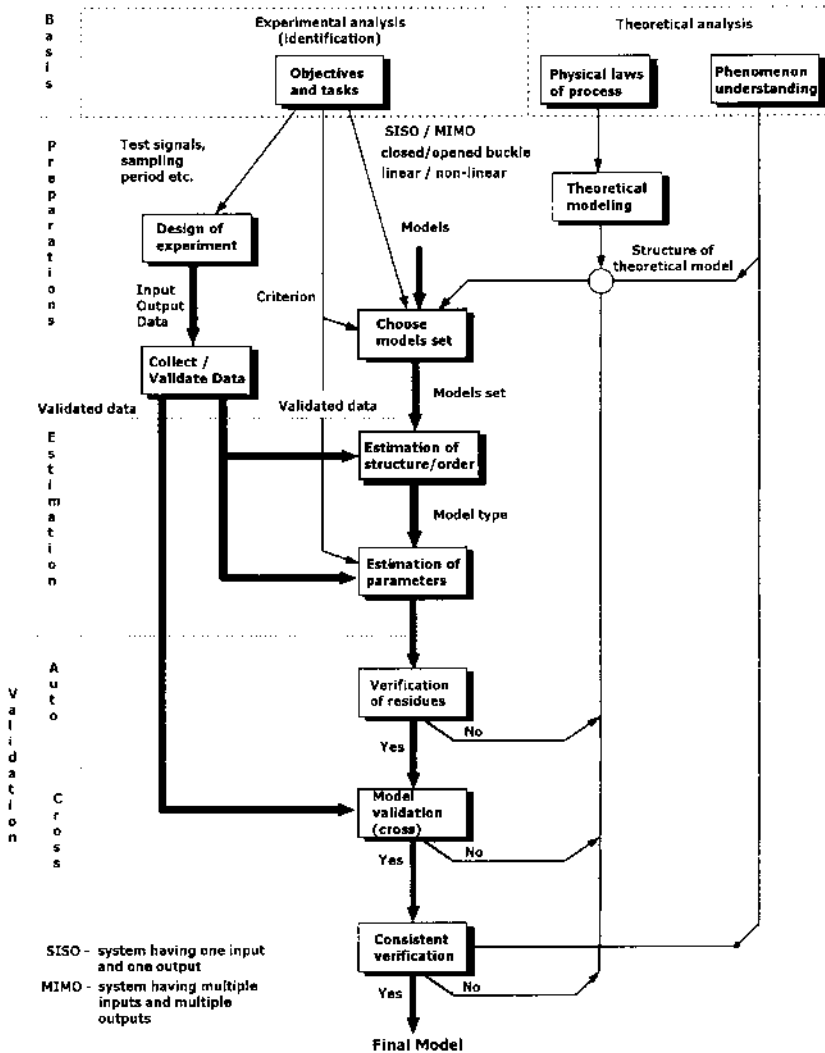


FIGURE 4.1 Combination of theoretical and experimental analyses.

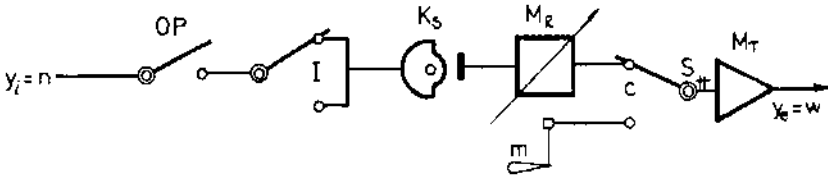


FIGURE 4.2 Classical structure of a kinematic feed chain.

The leading screw (which has a step of 10 mm and a double nut with balls ($D = 60$ mm, $d = 30$ mm, $p = 10$ mm, $z = 103$ bile, $D_w = 6$ mm, and $k_{Rb} = 12 \cdot 10^4$ daN/mm) to compensate the axial play) is fitted in two identical bearing cases that contain a pair of axial bearings 51307-P5 and one pair of radial bearings 6207-P6.

The slide movement along the body's guidings is ensured by the cam followers with rolls type GRT 3 ($L_w = 14$ mm, $C_o = 10200$ daN, $f = 1,25 \mu\text{m}$ at 1000 daN, $k_{cr} = 80 \cdot 10^3$ daN/mm), mounted in "O".

The material used for slide and body is cast iron (Fmn having $E = 1,6 \cdot 10^4$ daN/mm, $G = 4,5 \cdot 10^3$ daN/mm, $\gamma = 7,3$ kg/dm³, $\alpha = 18 \cdot 10^{-6}$ grd⁻¹) and the leading screw is made from alloyed steel (40Cr10 having: $E = 2,1 \cdot 10^4$ daN/mm, $G = 8,1 \cdot 10^3$ daN/mm, $\gamma = 8,2$ kg/dm³, $\alpha = 0,16 \cdot 10^{-6}$ grd⁻¹).

The block schema from Figure 4.4 highlights the main component elements of the mechanic stand.

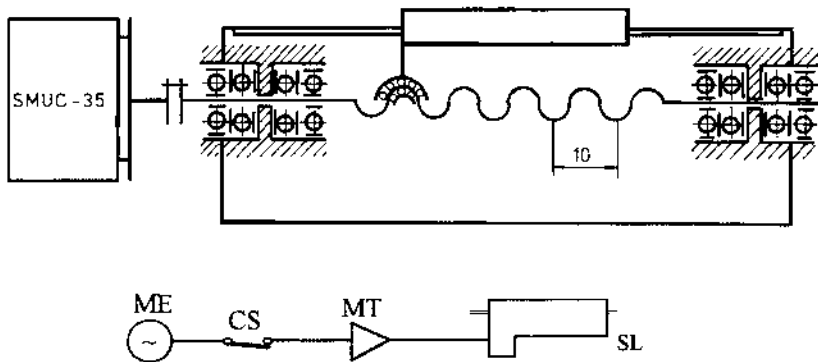


FIGURE 4.3 Structural kinematic schema of the studied kinematic feed chain.

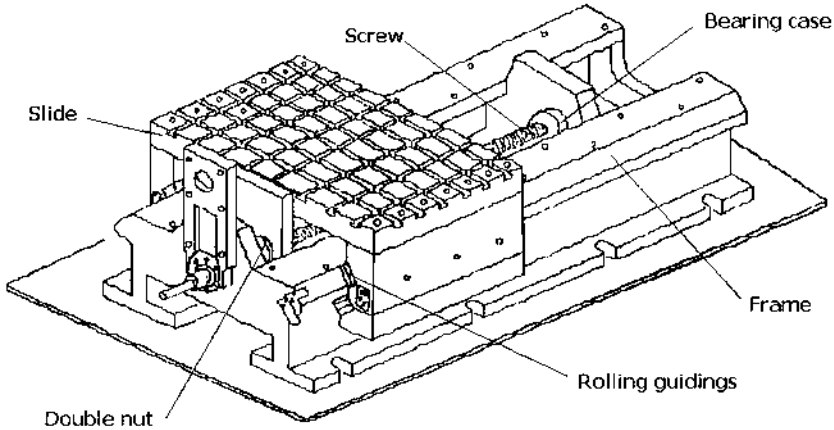


FIGURE 4.4 Main constitutive elements of the mechanical stand.

4.3 THEORETICAL ANALYSIS OF THE KINEMATIC FEED CHAIN MECHANICAL SYSTEM

The numerical analysis method proposes to model the physical phenomena in equations and describes the behavior of the physical systems by equations that express laws of mass, impulse, and shape conservation.

Finite difference methods consist of replacing the differentials from the equations of the model with very small finite differences, with the restriction of the validity only in certain points of the analyzed domain (the points of the discretized network of the model). Because of this method the discretized network will have a rectangular shape, thus for models with curved surfaces the method will be very difficult to apply.

Finite element methods (FEM) are based on local approximation, and on portions or subdomains that also consider the reports of relative dependence between the entire domain and the studied subdomain. The behavior of such a cut-up finite element is formulated by the equation:

$$[k] * \{d\} = \{q\} \tag{4.1}$$

where $[k]$ is the stiffness matrix of the finite element, $\{d\}$ is the vector of displacements from nodal points, and $\{q\}$ is the vector of the generalized forces that act on the elements by nodes.

The boundary element method (BEM) supposes that displacements produced by an elastic concentrate force applied at the origin (node) are known. This method is based on the equality between the mechanical work which results from the motion of a force system on the movement coordinates of a second force system and the mechanical work produced by the second system on the movements of the first. By using the relations between forces and displacements the tensor components that actually represent the problem's solution can be determined.

Among these three methods, the finite element method is most preferred because of the following qualities: large domain of applications, liberty to choose the type of discretization and to use simultaneously many more types of finite elements, discretization with variable geometry, and the possibility of performing calculus on substructures. The finite element method represents the "brick" of the discretized physical system, the shape, the type, and its equations being the discretization principles result.

4.3.1 The Method and Images 3D Algorithm

The FEM operates with three types of finite elements that are justified by geometry and number of independent coordinates:

Unidimensional elements (bar type), that have as ends even the nodes of the discretization network.

Bidimensional elements (plate type). The IMAGES 3D program includes two elements of this type: membrane (bending stressed only) and plate, which also has the thickness of the plate defined.

Tridimensional elements (prism, tetrahedral, and hexahedral type).

The increase in number of elements leads generally to the increase of the precision degree. However, over a certain value, the error does not decrease, no matter to what degree the number of the discretization elements would increase.

Interpolation functions are used to write the relations concerning the deformation and stress state of the finite element. The most used interpolation function is the Hermite function. For each type of finite element the rigidity matrix is determined (on the basis of the principle of virtual mechanical work), in the local axis system. This rigidity matrix is used to express finite element behavior by the known equation: $[k] * \{u\} = \{r\}$.

The assembling operation of the rigidity matrices and of the nodal force vectors determines the system of equations that characterize the structure: $[K] * \{U\} = \{R\}$, where the relation's terms represent the result of the aligning of the rigidity matrix and displacement and forces from the local system to the global axis system.

In order to ensure the convergence of solutions to the most exact solution, certain conditions must be followed.

The displacement models should be continuous inside the finite element. This condition is accomplished by the use of Gauss polynomial interpolation, which represents continuous functions. The displacements of the finite element should be compatible with the other ones. The displacement compatibility is satisfied only if the displacements of the points from every edge depend only on the displacements of the nodes that delimit the respective edge.

The displacement models should consider the displacements of the entire discretized system and also the constant stress state of elements. This supposes avoidance of a very fine discretization because when constructing the rigidity matrix, the elements of the main diagonal will be of negligible value (zero), which leads to a null determinant and thus to a wrong value of the inverse of this matrix.

4.3.2 Discretization of the Physical Model

The theoretical working model was obtained applying the similitude theory for the physical model presented. The reduction scale for the length was chosen as $\lambda = 2.5$ and the other scales have resulted:

$$\begin{aligned}\lambda_l &= \lambda_\varphi = \lambda_\delta = 2.5 \\ \lambda_E &= \lambda_G = \lambda_\sigma = \lambda_\mu = 1 \\ \lambda_F &= \lambda_l^2 = 6.25\end{aligned}\tag{4.2}$$

In other words: using the same material, the linear dimensions of the system are multiplied by λ , the forces by λ^2 , and the elastic constants are multiplied by λ for translation and by λ^3 for rotation, then the amplitudes and the frequencies are multiplied by λ , and the efforts remain unchanged.

The following discretization of structure was obtained (Fig. 4.5) based on the principles presented in the previous paragraph. The body

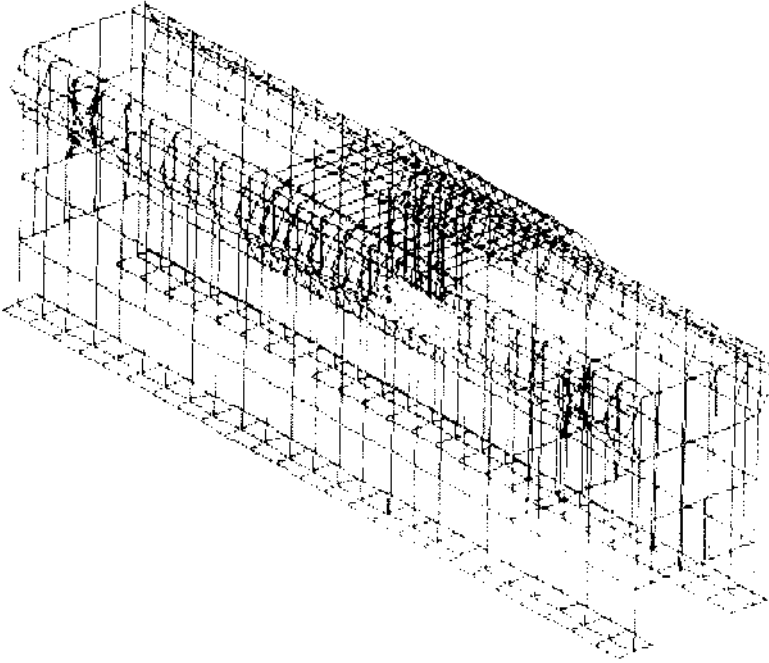


FIGURE 4.5 Structure discretization.

was made with a network of 613 points, the base finite element being the plate (membrane plates bending) under loads of compression and/or bending. The discretization is finer in the bearing zone to better estimate the maximum stress points of the structure.

The body guidings are also plate elements type, but they do not have a median longitudinal point that represents the contact point with the roll cam follower. This point has been connected to the extreme points of the finite element by springs with an increased rigidity compared to the other elements ($k = 10^7$ daN/mm). In this manner, the guiding-rollers contact is better approximated. Finally, for the longitudinal body and its guidings, 463 plates with a thickness between 20 and 40 mm have resulted.

The longitudinal slide (the table) was discretized using a step of 15 mm and 120 elements of plate type have resulted. The table's rolling guidings had been "replaced" by spring type elements having the same rigidity as the elements that define the link between the body and the

guiding plates. The leading screw was discretized in only 23 points because of its homogeneity and its physico-mechanical characteristics which are constant in all directions; a bar network that can be loaded to tensile and compression stresses results.

A tubular shaped nut was made using tridimensional finite elements (solids), which were connected to the table slide by means of plates made from the same material.

A special problem was the connection between the body and ground, which was made by springs connected to the ground, having in count the damping and elastic characteristics of the base material.

4.3.3 Statistical Analysis of Physical Model

Static loads were applied in order to determine the deformation mode of the mechanical system, a system designed as an assembly of elements that introduce deformations in a certain proportion for each element, and also to determine the zones of the structure having maximum deformations. In order to find the deformation mode, the load of the model's slide during the cutting process was simulated. The load was made with a static force that cumulated the weight of the semiproduct and the maximum value of the cutting force. The force was applied punctually on the slide decomposed on the following three directions: 1000 daN on OX; 2000 daN on OY; and 3000 daN on OZ. The total deformations of the constitutive elements were supervised on the above-mentioned three directions.

Studying the displacements on the OX axis, it has been observed that the most considerable yield ($\Delta x_{\max} = 1.14 \mu\text{m}$) is produced in the screw-nut mechanism, as expected. [Figure 4.6](#) presents a cut-through model to visualize the deformations to this mechanism. Less important deformations have resulted on the OY direction until $\Delta y_{\max} = -0.447 \mu\text{m}$ value (compression) in the guidings zone.

Hook's law can be applied to the entire model because the loading does not surpass the elastic domain. This law introduces the proportionality relation between the unitary efforts and the deformations. As a result, the tensor of unitary efforts may be calculated and represented using the same algorithm.

As previously mentioned, the deformation state was maximum at the screw-nut mechanism, so the nut stresses have been detailed as the element with the most important yield. Considering the global stress state it can be noticed that a maximum value $\sigma_{\max} = 4.51 \cdot 10^{-2} \text{ daN/mm}^2$ is

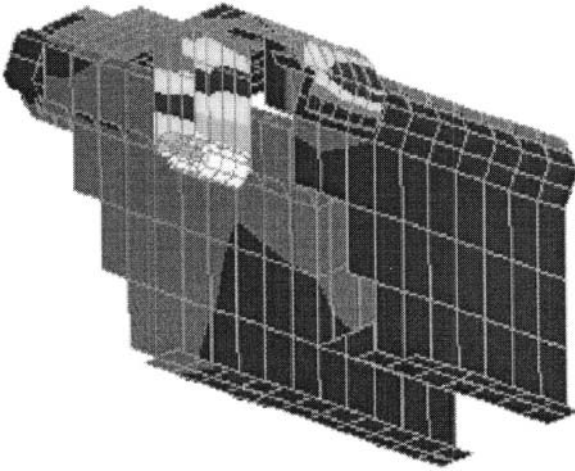


FIGURE 4.6 Section-through model.

reached. The analysis continued by decomposing the tensor on the main directions ($\sigma_{11}, \sigma_{22}, \sigma_{33}$ components). σ_{11}, σ_{22} have close values, but σ_{33} surpasses them by 150%, being by far most important (the maximum tensile strength: $\sigma_{33, \max} = 3.86 \cdot 10^{-2} \text{ daN/mm}^2$).

Figure 4.7 presents the global stress state of the physical model. It is evident that the maximum stresses are in the zone of the movement transform mechanism and the guidings zone; the body appears nonstressed but the table slide is stressed in the rolling guidings zone and at corners.

4.3.4 Modal Analysis of Physical Model

The method of modal analysis follows to determine certain dynamic characteristics by the estimation of the weights matrix, rigidity matrix, and damping matrix. As a result of this analysis the natural pulsations of the structure, the existent damping in the system, and the type of natural vibration modes can be deduced. The first three natural vibration modes and their corresponding natural frequencies were highlighted for the analyzed physical model using the IMAGES 3D program.

The first natural vibration mode (Fig. 4.8) affects the mechanism of movement transformation type screw-nut with balls and corresponds to a natural frequency of 259.6 Hz. High deformation of the free end

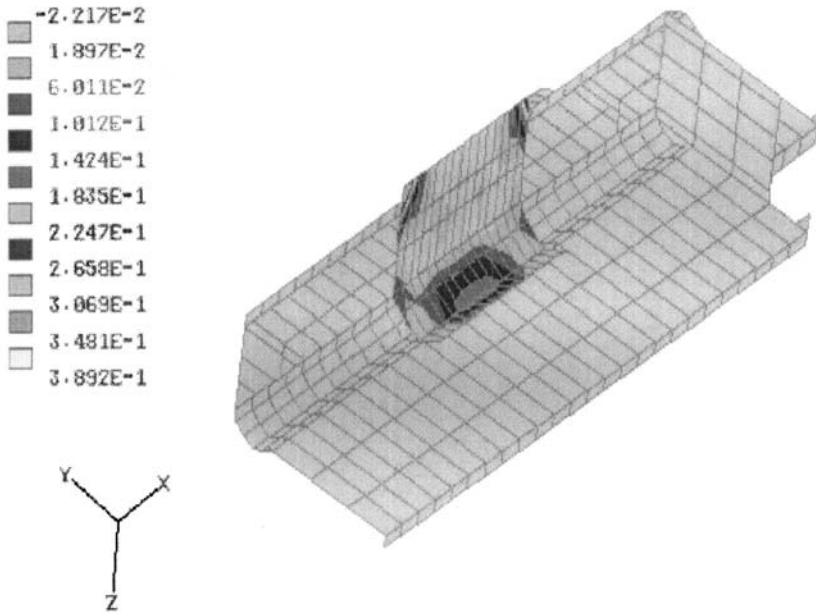


FIGURE 4.7 Global stress state of physical model.

of the nut is observed during the other subassemblages of the model (longitudinal slide, bearings, and body) to remain practically immobile.

The second natural vibration mode appears at 380 Hz frequency (Fig. 4.9), where a sensible deformation of the screw-nut mechanism is recorded, a slightly longitudinal and transversal deformation of guidings occurs, and a little transversal deformation of the body also occurs.

The third natural vibration mode (Fig. 4.10) occurs at 491 Hz and leaves the screw-nut mechanism almost undeformed. However, a powerful deformation of the guidings in a vertical direction and a slight deformation of the table slide are recorded.

The following conclusions can be formulated as a result of theoretical analysis of the mechanical system of the kinematic feed chain.

The most important yield from the kinematic feed chain belongs to the movement transforming mechanism.

The nut represents the most stressed element from the point of view of tension intensity.

The bearings rigidity influences the static and modal behavior of the leading screw.

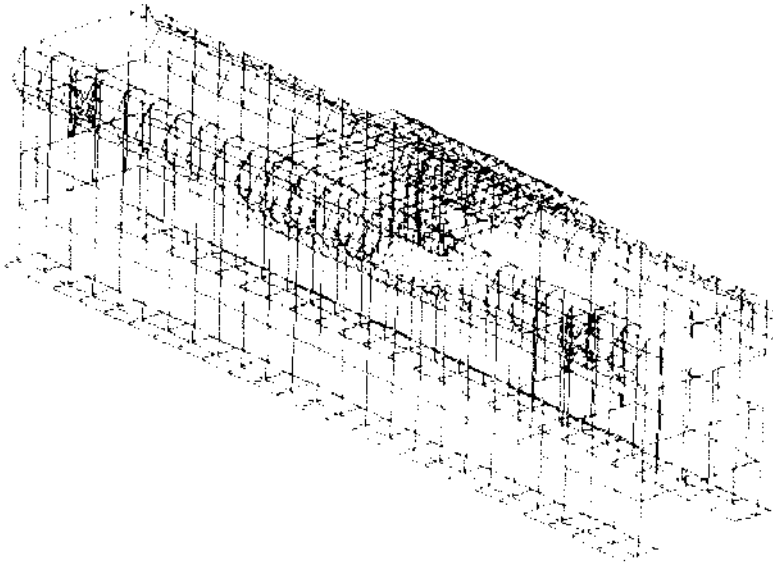


FIGURE 4.8 First natural vibration mode.

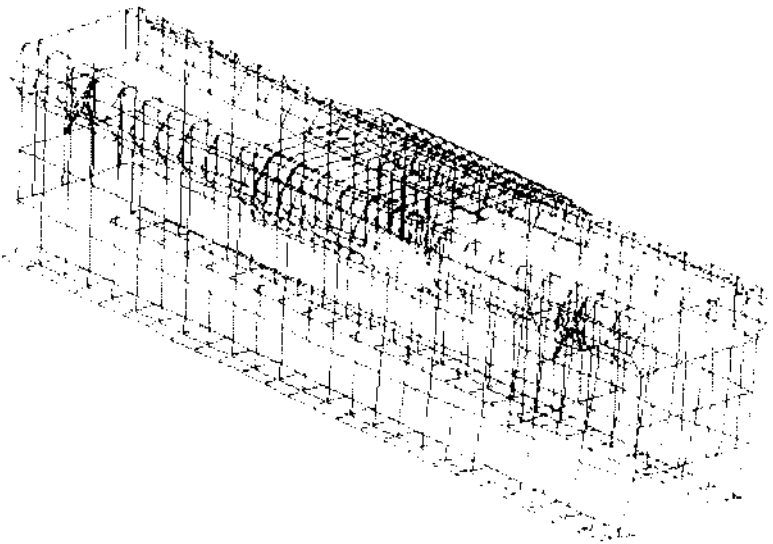


FIGURE 4.9 Second natural vibration mode.

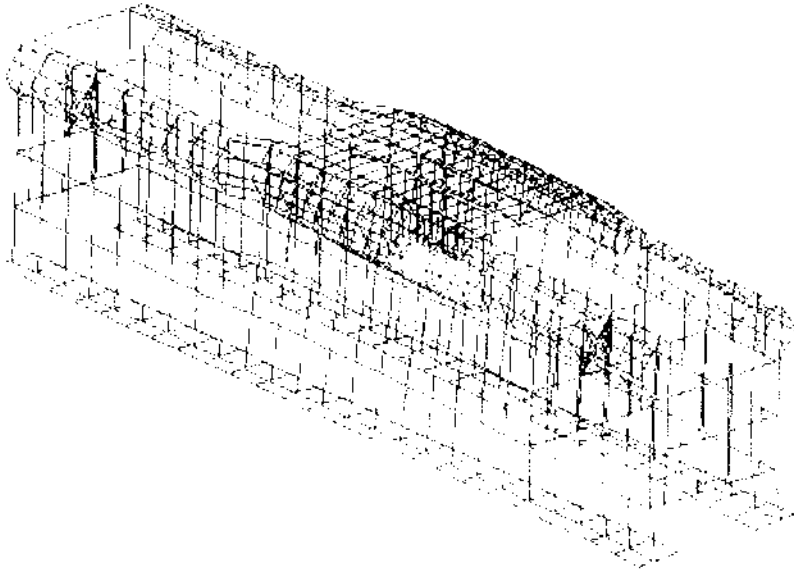


FIGURE 4.10 Third natural vibration mode.

The displacements of the slide-guidings-transforming mechanism ensemble are of major importance on transversal direction and less important on longitudinal direction.

The theoretical model constructed approximates with very good results the real model of the feed kinematic chain of a milling and reaming machine AF 180.

The FEM is susceptible to any factors that contribute to improvement of static and modal behavior of the analyzed structure.

The analysis led to the identification of the elements with maximum stresses in the structure, in order to monitor them during operation.

4.4 EXPERIMENTAL ANALYSIS OF KINEMATIC FEED CHAIN MECHANICAL SYSTEM

The vibration of a mechanical system is caused by external loadings or imposed movements that are variable in time, and are generally called

excitations or perturbations. Movements of different points of the system and the dynamical efforts from its elements are manifestations of the mechanical nature of these perturbations, and are called responses. The response is conditioned both by the excitation parameters and the mechanical characteristics of the system. Solving the vibration problems consists of establishing relations among excitation, response, and mechanical characteristics of the system.

The experimental analysis (identification) of the mechanical system proposes a series of functions of excitation and corresponding functions of response, to facilitate a mathematical description or an analytical model of the system. The relations between excitation and response are experimentally determined; the most frequently used data are the response curves in the frequency of the system obtained by excitation with test signals. On the basis of these curves, the identification of natural frequencies and vibration modes is made, and also of the specific dynamic properties. It is important that during experimentation the influence of other disturbing sources is reduced to a minimum. In addition the equipment used for structure excitation and response measurement should not modify the utilized mechanical system parameters.

The properties determined under these conditions sometimes differ from those obtained during normal functioning, especially in nonlinear structure cases. Choosing correct types and levels of excitation leads to satisfying results. The dynamic characteristics of a linear system with a single input $x(t)$ and a single output $y(t)$, can be described in the time domain by the proportion function $h(t)$, and in the frequency domain by the response in frequency function $H(i\omega)$ that constitute a pair of Fourier transforms:

$$H(i\omega) = \int_{-\infty}^{\infty} h(t)e^{-i\omega t} dt \quad (4.3)$$

In the case of determinist excitation, the response is given by the integral of convolution:

$$y(t) = \int_0^t h(t') x(t-t')d't = x(t) * h(t) \quad (4.4)$$

In this case the proportion function $h(t)$ represents the response to an excitation such as unity impulse (Dirac) $x(t) = \delta(t)$. The following relation gives the function response in frequency:

$$H(i\omega) = Y(i\omega)/X(i\omega) \quad (4.5)$$

where X and Y are the Fourier transforms of excitation and response, which can be written as

$$X(i\omega) = \int_{-\infty}^{\infty} x(t)e^{-i\omega t} dt \tag{4.6}$$

$$Y(i\omega) = \int_{-\infty}^{\infty} y(t)e^{-i\omega t} dt$$

the inferior limit being zero or the real systems.

If the structure excitation has been made with a force of the harmonic type, the $x(t)$ and $y(t)$ functions will have the expression:

$$x(t) = x_v e^{i\omega t}, \quad y(t) = y_v e^{i(\omega t + \varphi)} \tag{4.7}$$

which makes the response in the frequency function become

$$H(i\omega) = \frac{y_v}{x_v} e^{i\varphi} \tag{4.8}$$

From the above relation a very important conclusion results: the module of response in the frequency function ($|H(i\omega)|$) can be obtained from the amplitude-pulsation characteristic ($y_v/x_v - \omega$); and φ is obtained from the phase-pulsation characteristic ($\varphi - \omega$).

These diagrams can be determined experimentally using the sinusoidal excitation of constant amplitude and variable frequency. The two characteristics can be drawn either dot by dot, making measurements at discrete frequencies in the stationary regime, or continuum, using a frequency scavenging slow enough to permit the establishment of the regime response for each frequency. Using a live frequency analyzer simplifies the gathering of responses, a single excitation signal being sufficient. The structure of frequency analyzers includes an analyzer for functions compartment at whose entrance the signals $x(t) = x_v \sin \omega t$, $y(t) = y_v \sin(\omega t + \varphi)$ are applied and a reference signal $z(t) = z_v \cos(\omega t)$. This compartment performs the following multiplication,

$$x(t)y(t) \frac{2}{x_v^2} = \frac{y_v}{x_v} \cos \varphi - \frac{y_v}{x_v} \cos(2\omega t + \varphi) \tag{4.9}$$

$$z(t)y(t) \frac{2}{x_v z_v} = \frac{y_v}{x_v} \sin \varphi + \frac{y_v}{x_v} \sin(2\omega t + \varphi)$$

where the constant terms represent the real and imaginary parts of the response in frequency function. Elimination of variable terms is made

with down-pass filters, making the mean of the products on an integer number of cycles of excitation.

Processing the signals that correspond to the two components, the analyzer displays the polar (Nyquist) diagram of the response in frequency for the mechanical system (Fig. 4.11). Graphical analysis of these diagrams, as proposed by Kennedy and Pancu [82], remains the most exact method for determination of the dynamic parameters and of the type of natural vibration modes of a complex structure. To do this analysis, each buckle of the diagram is approximated with a circle and calculus relations established for systems with a single degree of freedom are used. Usually the work is done with the hypothesis of a proportional damping and, it is considered that, in the vicinity of no matter what natural frequency, the contribution of the nonresonator modes is either negligible, or constant (independent of the excitatory pulsation).

Localization of the natural pulsation is made, in this case, using the criterion of extreme value of the imaginaryary component of the diagram. Thus, the M point is found (the extreme point on the imaginary axis), and, corresponding to it, the ω_r frequency.

To determine the damping, the BC diameter is drawn perpendicular on $O'M$; this diameter intersects the approximation circle in

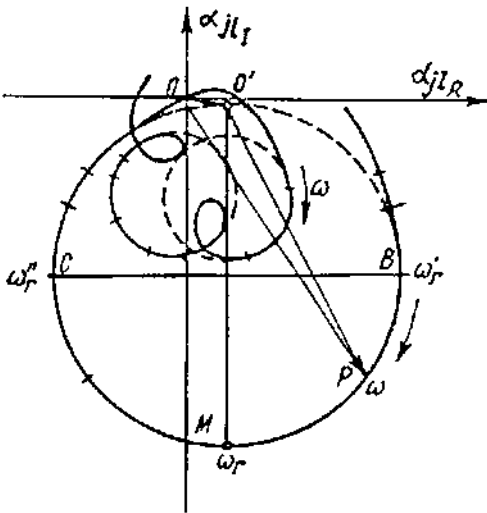


FIGURE 4.11 Polar (Nyquist) diagram.

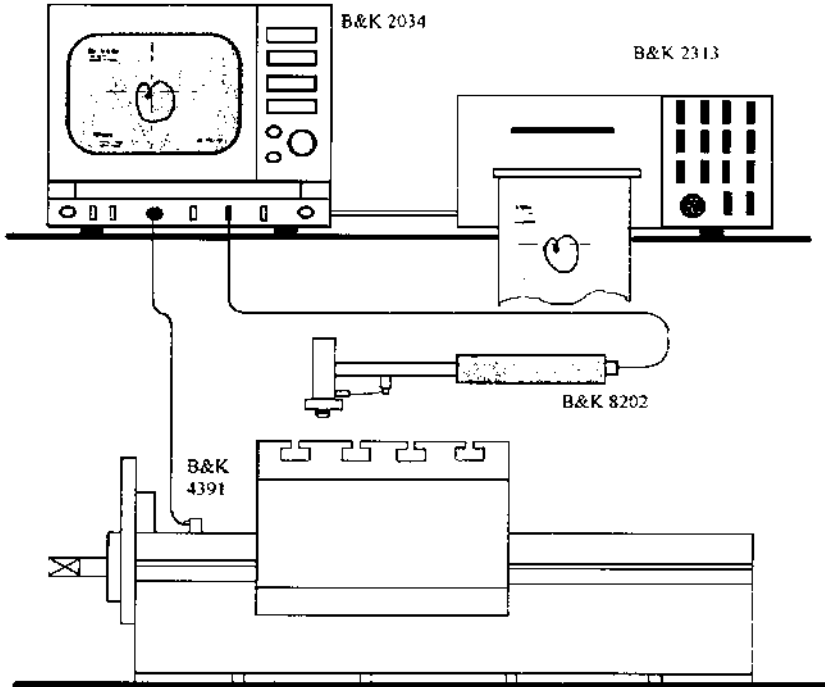


FIGURE 4.12 Experimental installation.

semipower points B and C , at $\omega_{r'}$ and $\omega_{r''}$ pulsations. The approximation factor is calculated with the equations:

$$g_r = \frac{\omega_{r''}^2 - \omega_{r'}^2}{2\omega_r^2} = \frac{\omega_{r''}^2 - \omega_{r'}^2}{\omega_{r''}^2 + \omega_{r'}^2} \quad (4.10)$$

The modal masses are calculated with the equation:

$$m_r = \frac{1}{\omega_r^2 g_r O'M} \quad (4.11)$$

The experimental analysis of the physical model of the kinematic feed chain followed the stages highlighted previously. The experimental installation used (Fig. 4.12) contained the impact hammer B & K 8202 and the real-time frequency analyzer B & K 2034. The model excita-

tion was made striking the longitudinal table in the vertical direction, and the structure response was captured from the body by a B & K 4391 accelerometer. The selected frequency domain was between 0 and 800 Hz, linear, considering the results of the theoretical analysis. Figure 4.13 presents graphics of the magnitude and phase of the response in frequency; it must be noticed that the maximum values are located at 265, 374, and 474 Hz in the magnitude/frequency graphic.

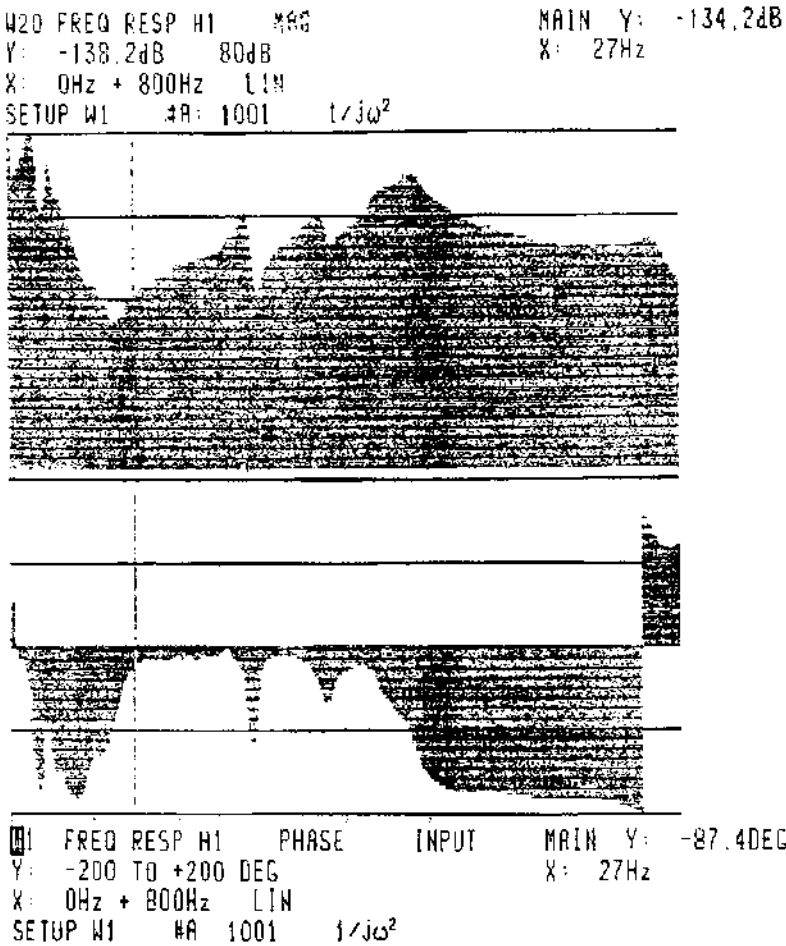
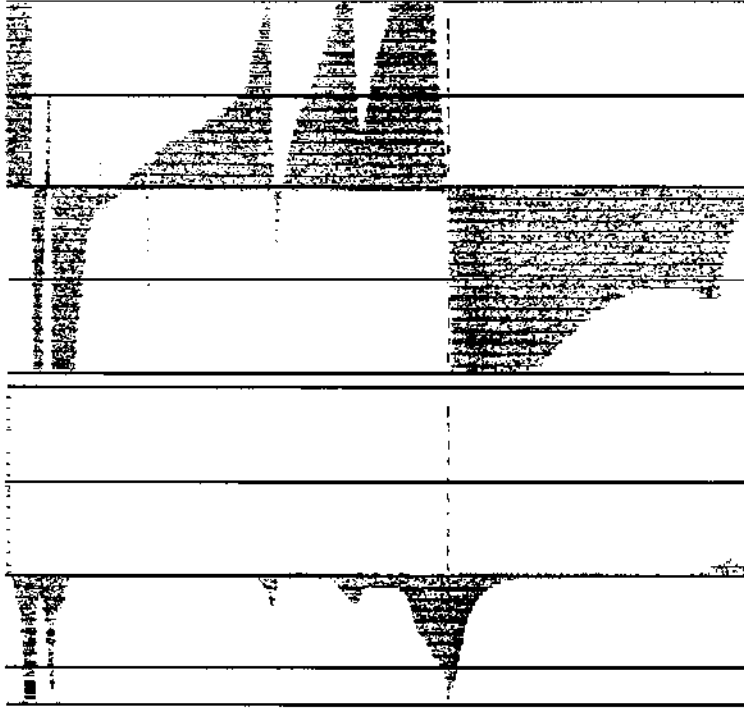


FIGURE 4.13 Graphics of magnitude and phase of the frequency response.

W20 FREQ RESP HI REAL
Y: 8.73E-9
X: 0Hz + 800Hz LIN
SETUP W1 #A: 1001 $1/j\omega^2$

MAIN Y: -774E-12
X: 474Hz



W1 FREQ RESP HI IMAG
Y: ~~8.73E-9~~
X: 0Hz + 800Hz LIN
SETUP W1 #A: 1001 $1/j\omega^2$

MAIN Y: -34 4E-9
X: 474Hz

FIGURE 4.14 Processed signal to obtain the real and imaginary components of the frequency response.

At the next stage, the signal was processed in order to obtain the real and imaginary components of the frequency response (Fig. 4.14). Nyquist diagram was then drawn using these components (Fig. 4.15). The results indicate a stable structure from the dynamical point of view, as expected from the theoretical analysis made by the finite element method. The differences between the calculated natural pulsations using the FEM and those experimentally obtained are minimal, as Table 4.1 shows.

The experimental validation of the natural frequencies and the implicit natural vibration modes estimated by the finite element method

```

W20 FREQ RESP HI    NYQUIST          MASK Y: -196E-9
Y: 196E-9           F: 270z
X: 392E-9           X: 9.22E-9
SETUP W]          #A: 1001    1/jω²   [ ]
  
```

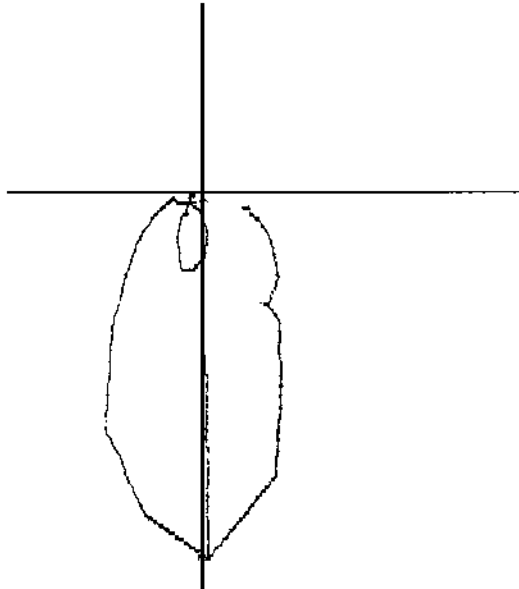


FIGURE 4.15 Nyquist diagram drawn using real and imaginary components of the frequency response.

TABLE 4.1 Differences Between Calculated Natural Pulsations Using FEA and Those Experimentally Obtained

| | | | |
|--|-------|------|------|
| Calculated natural frequency, f_c [Hz] | 259.6 | 380 | 491 |
| Measured natural frequency, f_m [Hz] | 265 | 374 | 474 |
| Deviation $\varepsilon = \left \frac{f_m - f_c}{f_m} * 100 \right $ [%] | 2.04 | 1.60 | 3.59 |

lead to the conclusion that the analysis methods implied by this research have been correctly applied, and the results obtained are significant.

4.5 CONCLUSIONS AND IMPLICATIONS OF DIAGNOSTIC ANALYSIS IN FUTURE RESEARCH

Theoretical and experimental analysis of the physical model of the kinematic feed chain have yielded the possibilities of identifying the points of maximum stress in the structure of the kinematic chain, and identifying the natural frequencies of the structure. In addition, reliable stability of the physical model has been confirmed, which makes this an apt model for the study of problems related to the technical diagnosis of elements from its structure.

By analyzing the deformations of the physical model the following highlighted that the most important yield occurs where the zone of the mechanism is predisposed to failures, namely, the transforming mechanism screw-nut with balls and the rolling guidings of the longitudinal slide. These yields can influence the functioning of the mechanism and speed up the occurrence of the damaging processes that contribute to the mechanism's failure. The deformation values are closer to those of the preadjusted mechanical plays in these mechanisms that can lead to a fault functioning.

Knowing the natural frequencies of the structure enables us to compare them with the characteristic frequencies (of operation) of all the mechanisms in the studied kinematic chain's structure. From the technical literature and also from the theoretical and experimental research for the determination of the characteristic frequencies of some mechanisms with bearings, ball screws, and roller cam followers, it has

been noticed that these work frequencies are in a neighboring domain with that of the investigated natural frequencies, but usually inferior.

Theoretically there is a possibility of resonance occurrence with the natural frequencies because of the important increase in the power spectrum (e.g., for an element with mechanical fault) that occurs not only at the characteristic frequencies, but also superior harmonics of these frequencies. This phenomenon leads to signals of false mechanical faults and unreasonable stoppages of machines, and happens especially in online diagnosis systems having low resolution.

The results of this diagnostic analysis have oriented, from these points of view, future theoretical and applicative research concerning technical diagnostics for some elements of the general structure of kinematic feed chains.